nature biotechnology

Targeted integration in rat and mouse embryos with zinc-finger nucleases

Xiaoxia Cui, Diana Ji, Daniel A Fisher, Yumei Wu, David M Briner & Edward J Weinstein

Gene targeting is indispensible for reverse genetics and the generation of animal models of disease. The mouse has become the most commonly used animal model system owing to the success of embryonic stem cell–based targeting technology[1], whereas other mammalian species lack convenient tools for genome modification. Recently, microinjection of engineered zinc-finger nucleases (ZFNs) in embryos was used to generate gene knockouts in the rat[2,3] and the mouse[4] by introducing nonhomologous end joining (NHEJ)-mediated deletions or insertions at the target site. Here we use ZFN technology in embryos to introduce sequence-specific modifications (knock-ins) by means of homologous recombination in Sprague Dawley and Long-Evans hooded rats and FVB mice. This approach enables precise genome engineering to generate modifications such as point mutations, accurate insertions and deletions, and conditional knockouts and knock-ins. The same strategy can potentially be applied to many other species for which genetic engineering tools are needed.

Conventional gene targeting in mouse embryonic stem (ES) cells is achieved by introduction of an antibiotic selection marker through homologous recombination. Targeted ES cells are then injected into wild-type blastocysts to generate chimeric animals, some of which contain targeted germ cells[5]. Time-consuming backcrossing is often necessary when ES cells are not available from the desired strain[5]. Moreover, in species without established ES cell lines, targeted gene modification is not feasible, largely limiting their use as model systems. For example, the rat is a preferred model over mice for studying many human diseases[6] but has lacked robust genetic modification tools until the application of ZFNs[2,3]. Although considerable progress has been made recently with rat ES cells[7,8], ZFN technology may overcome the limitations of ES cell technology.

ZFNs generate sequence-specific double-strand breaks[9,10] that are repaired mainly by either error-prone nonhomologous end joining (NHEJ) or high-fidelity homologous recombination (**Supplementary Fig. 1**). Embryonic injection of ZFNs has produced NHEJ-mediated knockout rats[2,3], mice[4] and zebrafish[11–13] with remarkable efficiency and germline transmission rates. However, mutations are unpredictable owing to the variable nature of DNA repair by NHEJ[14] and are limited to knockouts. On the other hand, successful homologous recombination in embryos using a homologous donor template provides accuracy and flexibility that the NHEJ process lacks, and enables gene addition.

Homologous recombination–mediated targeted integration was observed in mouse embryos after injection of donor DNA into eggs at a rate of <0.2%[15]. ZFN-mediated double-strand breaks have been shown in cultured human cells[16–18] and flies[19] to stimulate homologous recombination by several orders of magnitude. We set out to test and successfully achieved robust ZFN-assisted homologous recombination in both rat and mouse embryos.

Based on previous data in human cell lines[16,18], we first constructed donors with an eight base pair (bp) NotI restriction site inserted in between the ZFN binding sites, flanked by ~800 bp of immediate homology on each side (**Fig. 1a** and **Supplementary Tables 1** and **2**). Donor plasmid DNA and respective ZFN mRNA were co-injected into the pronucleus of one-cell embryos from Sprague Dawley rats and FVB mice followed by transfer of the injected eggs to pseudo-pregnant females.

Fetuses of NotI donors were harvested for analysis. Integration of the NotI site was detected using NotI digestion of PCR products of the target region amplified with primers outside of the homologous arms (F and R as shown in **Fig. 1a**). **Figure 1b** shows the expected digestion pattern of NotI integration in fetuses at the rat *Mdr1a* (1 of 15 13-day-old Sprague Dawley rat fetuses) and *PXR* loci (1 of 8 14-day-old Sprague Dawley rat fetuses) and the mouse *Mdr1a* locus (1 of 4 12.5-day-old FVB mouse fetuses). Sequencing of the PCR products confirmed the presence of a NotI site in all three loci, as well as deletions by NHEJ at both rat and mouse *Mdr1a* loci (**Supplementary Fig. 2**), indicating that these fetuses were mosaics. In addition, the *Mdr1a* locus was also successfully targeted in Long-Evans hooded rats. One of seven pups was identified as a founder (**Supplementary Fig. 3**), harboring two alleles: NotI insertion in one and an 11-bp deletion in the other. When the founder was bred to a wild-type Long-Evans hooded rat, 5 out of 12 F1 pups inherited the NotI allele, and 7 contained the 11-bp deletion allele.

Next, we constructed GFP donors, replacing the NotI site with a 1.5-kilobase (kb) human phosphoglycerate kinase (PGK) promoter-driven GFP cassette (**Fig. 2a** and **Supplementary Tables 1** and **2**). GFP is in the opposite orientation of transcription for the rat *Mdr1a* and *PXR* loci and the same orientation of transcription at the mouse *Mdr1a* locus. We analyzed live-born pups of GFP donors. DNA extracted from toe clips was amplified in four PCR reactions using primer sets (i) GF and GR, (ii) F and R, (iii) F and GF and (iv) R and GR (**Fig. 2a**). Set (i) amplified the GFP cassette, whereas set (ii) amplified the target region, favoring wild-type, deletion and small-insertion alleles over

Sigma Advanced Genetic Engineering (SAGE) Labs, Sigma-Aldrich Biotechnology, St. Louis, Missouri, USA. Correspondence should be addressed to X.C. (xiaoxia.cui@sial.com).

Received 9 April; accepted 10 November; published online 12 December 2010; doi:10.1038/nbt.1731

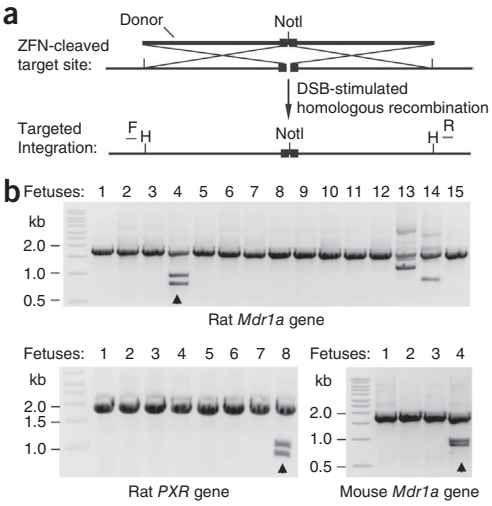

Figure 1 Targeted integration of NotI restriction site. (**a**) Schematic of donor and target site. Donors contain a NotI site inserted between the ZFN binding sequences (squares) with two flanking 800 bp homologous arms. F and R, forward and reverse primers (short bar) that sit outside of the homology. H, boundary of homology. DSB, double-strand break. (**b**) One pup (arrowhead) with NotI insertion was identified in each target using PCR with specific F and R primers followed by NotI digestion.

the targeted integration allele that is 1.5 kb larger than the wild type and rarely amplified by F and R primers when other alleles are present. Set (ii) also served as a positive control for genomic DNA quality. Sets (iii) and (iv) amplified the 5′ and 3′ respective junctions specific to targeted insertion and were the diagnostic reactions for targeted integration events. Expected product sizes are listed in **Supplementary Table 2**. **Figure 2b** shows that *Mdr1a* pup no. 3 and *PXR* pup no. 4 were positive for GFP and both junctions and contained the targeted insertion, whereas *Mdr1a* pup no. 19 was positive for GFP only, thus carrying a transgene. Sequencing revealed that *Mdr1a* pup no. 3 was a mosaic with three alleles: the targeted integrant and deletions of 513 bp and 6 bp, respectively (**Supplementary Table 3**). The complete panel of PCR reactions is shown in **Supplementary Figure 4**. NHEJ events in the pups were further analyzed (**Supplementary Fig. 5**). Using the same donor configuration, the mouse *Mdr1a* locus was targeted at 5% efficiency (**Supplementary Fig. 6**). The sequences of all junction PCR products were validated.

Southern blot analysis further confirmed integration of the GFP cassette to the target loci. Both flanking and internal probes were used. The flanking target probes (labeled as Mrd1a and PXR, respectively) were located outside of the homologous arms and hybridized to all alleles, whereas the internal probe (GFP) detected the GFP cassette (**Fig. 2a**). At the rat *Mdr1a* locus, the GFP probe recognized a single 4.5-kb band corresponding to targeted integration in pup no. 3 but not in the wild type (**Fig. 2c**), demonstrating that the GFP cassette was specifically inserted into the desired site, whereas the *Mdr1a* probe detected a single wild-type band of 3 kb in the wild-type sample, and three bands in pup no. 3, corresponding to the integration allele (4.5 kb), and the alleles with 6- and 513-bp deletions, respectively. PGK-GFP was expressed and visually detectable in the eyes of founder no. 3 under UV light (**Fig. 2d**). Founder no. 3 was then mated to a wild-type Sprague Dawley male. Approximately 50% of the F1 offspring inherited the targeted integration allele (**Fig. 3a**, **Supplementary Fig. 7** and **Supplementary Table 4**). Mating between integration-positive F1 animals generated homozygous F2 offspring that appeared normal. Southern blot analysis of the F2 animals is shown in **Figure 3b**.

For *PXR* founder no. 4, the flanking probe recognized two bands corresponding to the wild-type (4.7 kb) and integration (6.2 kb) alleles (**Fig. 2c**). However, there is an extra band around 4 kb hybridizing to the GFP probe that could have resulted from random integration (as in *Mdr1a* pup no. 19). When founder no. 4 was mated to wild-type Sprague Dawley females, ~50% of the F1 offspring was heterozygous for the GFP targeted integration allele, some of which also inherited the extra GFP locus. But the majority of F1 animals contained only the targeted integration allele (**Fig. 3c** and **Supplementary Table 4**).

Additional injection sessions produced another *Mdr1a* founder, no. 4-5, and two more *PXR* founders, no. 2-1 and no. 2-2 (**Supplementary Table 3** and **Supplementary Fig. 8**). Founder no. 4-5 contained a 147-bp deletion in addition to the targeted integration allele. Founder no. 2-1 contained a targeted integration allele and a wild-type allele. Normal breeding yielded ~50% F1 offspring heterozygous for the targeted integration allele (not shown). Founder no. 2-2 contained the targeted integration allele, an allele with a 236-bp deletion and an extra GFP locus.

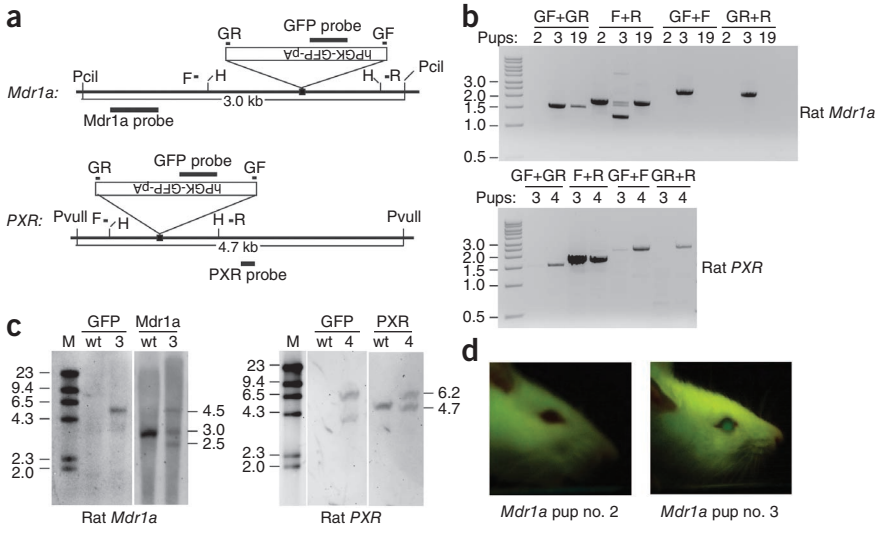

Figure 2 Targeted integration of a GFP cassette. (**a**) Schematic of target site (square) and GFP integration at *Mdr1a* and *PXR* loci. F, R and H, same as in **Figure 1a**. GF and GR, forward and reverse primers in GFP cassette. PvuII and PciI are restriction enzymes used in Southern blot analysis; neither cuts the 1.5-kb GFP insert, which inserts in the opposite orientation of transcription in both donors. Probes used in Southern blot analysis (thick bars) are marked at corresponding positions. (**b**) PCR analysis of GFP integration in selected *Mdr1a* and *PXR* rat pups. Pup IDs are labeled under the primers used. (**c**) Southern blot analysis of pups for GFP integration. GFP, GFP probe; Mdr1a and PXR, respective flanking probes. wt, wild-type Sprague Dawley genomic DNA. (**d**) GFP expression was visualized under UV light in the eyes of *Mdr1a* founder no. 3. Full-length blots are presented in **Supplementary Figure 9**.

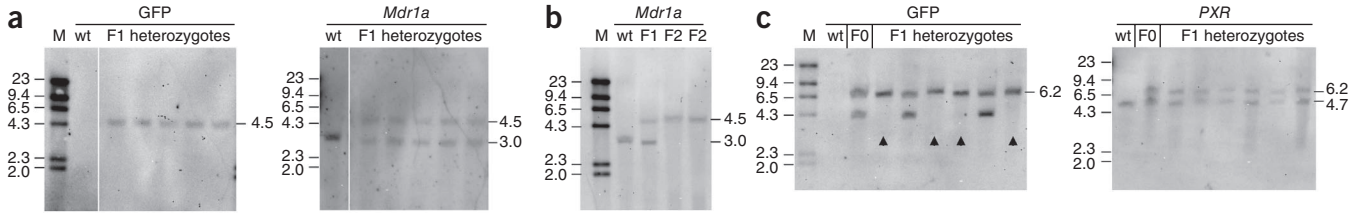

Figure 3 Germline transmission of site-specific GFP integration. Integration-positive offspring of *Mdr1a* founder no. 3 (F1 and F2 pups identified by PCR as in **Supplementary Fig. 7a** and not shown) and *PXR* founder no. 4 (F1 pups identified by PCR as in **Supplementary Fig. 7b**) were further confirmed with Southern blot analysis. GFP, GFP probe; Mdr1a and PXR, respective target probes. wt, wild-type Sprague Dawley genomic DNA. (**a**) *Mdr1a* heterozygotes. (**b**) *Mdr1a* F2 homozygotes. Wild-type and an F1 heterozygote are included as controls. (**c**) *PXR* F1 heterozygotes. Arrowheads indicate F1 animals in which targeted integration allele of *PXR* was segregated from the extra GFP locus. Full-length blots are presented in **Supplementary Figure 9**.

Table 1 summarizes the injection statistics that support the following conclusions: first, offspring of animals co-injected with ZFN mRNA and donor plasmid had similar overall survival and live-birth rates, as previously reported[2,20], indicating minimal toxicity. In addition, mutant animals appeared to be physically normal and bred well, except for *PXR* founder no. 2-2, which developed hydrocephalus of unknown cause and had to be euthanized. Second, NHEJ occurs at a higher rate than targeted integration. Thus, the presence of NHEJ-positive pups among live births should be used as a criterion for a successful injection session. For example, between *Mdr1a*/GFP and *PXR*/GFP injections, four sessions failed to produce founders with targeted integration, three of which did not generate any NHEJ-positive pups, implying possible variance in sample preparation and/or injection. **Table 1** combined data from all sessions, including those that probably failed.

Mosaicism is common among mutant animals produced with ZFNs and has been observed in knockout rats[2,3] and mice[4], where up to five different alleles were detected in individual founders. **Supplementary Table 3** summarizes the genotype of all targeted, integration-positive animals generated in this study, some of which contained up to three alleles. The degree of mosaicism in the founders likely correlates to the length of time ZFNs remain active in the embryos. Each cell division doubles the number of existing targetable (wild-type) alleles, allowing more independent NHEJ events to create different mutant alleles. In founders carrying more than two alleles, ZFNs must remain functional beyond the one-cell embryo stage.

Germline transmission of NHEJ-modified and targeted integration alleles is highly efficient. All alleles identified in founders *Mdr1a* no. 3 and *PXR* no. 4 were inherited in the F1 generation (**Supplementary Table 4**). The high germline transmission rate is consistent with the fact that mosaicism develops in embryos containing only a few cells, all of which have the potential to become germ cells, including those carrying alleles with low representation in the body. For example, sequencing of the PCR products in **Figure 2b** identified a 35-bp deletion only at the *PXR* locus with no wild-type allele in founder no. 4. However, 2 of the 57 F1 pups were wild type (**Supplementary Tables 3** and **4**). Overall, allele distribution among F1 offspring correlated roughly to the relative ratio among alleles detected in Southern blot analysis (**Fig. 2c** and **Supplementary Table 4**).

To our knowledge there has been no previous report of robust targeted integration in rat embryos of different backgrounds and complete germline transmission. While this manuscript was in revision, another group reported a similar targeting strategy in mice[21]. The same method may enable one to introduce precise modifications, such as point mutations, specific insertions and deletions, gene replacement, conditional knock-ins and knockouts, to an exact locus directly in embryos that then develop into mutant animals. Nevertheless, there are potential limitations to ZFN technology. Primarily, ZFNs have yet to be engineered to target any given sequence, which may limit the ability to introduce mutations at loci lacking ZFN target sites in the vicinity. Continuous improvement of ZFN design is necessary. Second, undesired modifications by ZFNs are also possible and have been detected at low rates in cultured human cells[22–24], although none have been observed in ZFN-engineered rodents so far[2–4]. In the meantime, advances in ZFN engineering continue to improve specificity[18,24–26]. In addition, unwanted mutations may segregate from the target loci and be eliminated from subsequent generations by breeding (**Fig. 3c** and **Supplementary Table 4**). Recently, the disruption of the p53 gene in a rat ES cell line and germline transmission were described[7]. In a separate report, germline transmission of a transgene was also demonstrated[8]. These are major improvements in ES cell technology that could help replicate in the rat the sophisticated targeting strategies that are already well developed in the mouse. However, ZFN technology possesses several advantages. First, ZFN-mediated homologous recombination in embryos does not require selectable markers. Second, the time frame needed to obtain mutant animals is shortened by bypassing ES cells and efficient germline transmission. More importantly, gene targeting using ZFN technology is not limited by the availability of ES cells, and time-consuming backcrossing is avoided. Finally, in theory, ZFN technology can be applied to any organism for which fertilized eggs can be collected, microinjected and transferred into pseudopregnant females.

Table 1 Injection statistics

Target	Donor	Strain	Embryos injected	Embryos transferred	Fetuses (f) or pups (p)	TI positive (mutation rate in %)	NHEJ positive (mutation rate in %)
Mdr1a	NotI	SD	97	81	15f	1 (6.7)	3 (2.0)
	MCS	LEH	125	80	7p	1 (14.3)	2 (28.6)
	GFP	SD	636	439	83p	2 (2.4)	21 (25.3)
	NotI	FVB	46	46	4f	1 (25.0)	3 (75.0)
	GFP	FVB	106	106	40f	2 (5.0)	3 (7.5)
PXR	NotI	SD	56	52	8f	1 (12.5)	3 (37.5)
	GFP	SD	670	472	36p	3 (8.3)	4 (11.1)

NotI: donor constructs with NotI site inserted in between the homologous arms (**Fig. 1a**). GFP: donor constructs with GFP cassette inserted in between the homologous arms (**Fig. 2a**). MCS: *Mdr1a* donor construct with multiple cloning site inserted in the NotI site in NotI donor. SD: Sprague Dawley rats; FVB, FVB/NTac mice; LEH: Long-Evans hooded rats. TI positive: the number of pups or fetuses harboring targeted integration; NHEJ positive: the number of pups or fetuses positive in mutation detection assay.

METHODS

Methods and any associated references are available in the online version of the paper at http://www.nature.com/naturebiotechnology/.

Note: Supplementary information is available on the Nature Biotechnology website.

ACKNOWLEDGMENTS

We thank J. Books for technical assistance; R. DeKelver at Sangamo Biosciences for GFP plasmid; A. Harrington and L. Liaw for mouse microinjections; Z. Cui, G. Davis and T. Saunders for discussion; D. Carroll, K. Cunningham, T. Collingwood and F. Urnov for suggestions; and S. Fine for excellent assistance with figures.

AUTHOR CONTRIBUTIONS

X.C. designed the project, built donor constructs and carried out some of the diagnostic PCRs; D.J. built donor constructs and performed most of the PCR diagnosis; D.A.F. performed Southern blot analysis; Y.W. microinjected the rat samples; D.M.B. assembled ZFNs; X.C., D.J., D.A.F. and E.J.W. wrote the manuscript.

COMPETING FINANCIAL INTERESTS

The authors declare competing financial interests: details accompany the full-text HTML version of the paper at http://www.nature.com/naturebiotechnology/.

Published online at http://www.nature.com/naturebiotechnology/.
Reprints and permissions information is available online at http://npg.nature.com/reprintsandpermissions/.

1. Capecchi, M.R. Gene targeting in mice: functional analysis of the mammalian genome for the twenty-first century. *Nat. Rev. Genet.* **6**, 507–512 (2005).
2. Geurts, A.M. *et al.* Knockout rats via embryo microinjection of zinc-finger nucleases. *Science* **325**, 433 (2009).
3. Mashimo, T. *et al.* Generation of knockout rats with X-linked severe combined immunodeficiency (X-SCID) using zinc-finger nucleases. *PLoS ONE* **5**, e8870 (2010).
4. Carbery, I.D. *et al.* Targeted genome modification in mice using zinc finger nucleases. *Genetics* **186**, 451–459 (2010).
5. Ledermann, B. Embryonic stem cells and gene targeting. *Exp. Physiol.* **85**, 603–613 (2000).
6. Aitman, T.J. *et al.* Progress and prospects in rat genetics: a community view. *Nat. Genet.* **40**, 516–522 (2008).
7. Tong, C., Li, P., Wu, N.L., Yan, Y. & Ying, Q.L. Production of p53 gene knockout rats by homologous recombination in embryonic stem cells. *Nature* **467**, 211–213 (2010).
8. Kawamata, M. & Ochiya, T. Generation of genetically modified rats from embryonic stem cells. *Proc. Natl. Acad. Sci. USA* **107**, 14223–14228 (2010).
9. Kim, Y.-G., Cha, J. & Chandrasegaran, S. Hybrid restriction enzymes: zinc finger fusions to Fok I cleavage domain. *Proc. Natl. Acad. Sci. USA* **93**, 1156–1160 (1996).
10. Mani, M., Smith, J., Kandavelou, K., Berg, J.M. & Chandrasegaran, S. Binding of two zinc finger nuclease monomers to two specific sites is required for effective double-strand DNA cleavage. *Biochem. Biophys. Res. Commun.* **334**, 1191–1197 (2005).
11. Doyon, Y. *et al.* Heritable targeted gene disruption in zebrafish using designed zinc-finger nucleases. *Nat. Biotechnol.* **26**, 702–708 (2008).
12. Meng, X., Noyes, M.B., Zhu, L.J., Lawson, N.D. & Wolfe, S.A. Targeted gene inactivation in zebrafish using engineered zinc-finger nucleases. *Nat. Biotechnol.* **26**, 695–701 (2008).
13. Foley, J.E. *et al.* Rapid mutation of endogenous zebrafish genes using zinc finger nucleases made by oligomerized pool engineering (OPEN). *PLoS ONE* **4**, e4348 (2009).
14. Lieber, M.R. The biochemistry and biological significance of nonhomologous DNA end joining: an essential repair process in multicellular eukaryotes. *Genes Cells* **4**, 77–85 (1999).
15. Brinster, R.L. *et al.* Targeted correction of a major histocompatibility class II E alpha gene by DNA microinjected into mouse eggs. *Proc. Natl. Acad. Sci. USA* **86**, 7087–7091 (1989).
16. Moehle, E.A. *et al.* Targeted gene addition into a specified location in the human genome using designed zinc finger nucleases. *Proc. Natl. Acad. Sci. USA* **104**, 3055–3060 (2007).
17. Porteus, M.H. & Baltimore, D. Chimeric nucleases stimulate gene targeting in human cells. *Science* **300**, 763 (2003).
18. Urnov, F.D. *et al.* Highly efficient endogenous human gene correction using designed zinc-finger nucleases. *Nature* **435**, 646–651 (2005).
19. Bozas, A., Beumer, K.J., Trautman, J.K. & Carroll, D. Genetic analysis of zinc-finger nuclease-induced gene targeting in *Drosophila*. *Genetics* **182**, 641–651 (2009).
20. Filipiak, W.E. & Saunders, T.L. Advances in transgenic rat production. *Transgenic Res.* **15**, 673–686 (2006).
21. Meyer, M., de Angelis, M.H., Wurst, W. & Kühn, R. Gene targeting by homologous recombination in mouse zygotes mediated by zinc-finger nucleases. *Proc. Natl. Acad. Sci. USA* **107**, 15022–15026 (2010).
22. DeKelver, R.C. *et al.* Functional genomics, proteomics, and regulatory DNA analysis in isogenic settings using zinc finger nuclease-driven transgenesis into a safe harbor locus in the human genome. *Genome Res.* **20**, 1133–1142 (2010).
23. Hockemeyer, D. *et al.* Efficient targeting of expressed and silent genes in human ESCs and iPSCs using zinc-finger nucleases. *Nat. Biotechnol.* **27**, 851–857 (2009).
24. Perez, E.E. *et al.* Establishment of HIV-1 resistance in CD4+ T cells by genome editing using zinc-finger nucleases. *Nat. Biotechnol.* **26**, 808–816 (2008).
25. Miller, J.C. *et al.* An improved zinc-finger nuclease architecture for highly specific genome editing. *Nat. Biotechnol.* **25**, 778–785 (2007).
26. Szczepek, M. *et al.* Structure-based redesign of the dimerization interface reduces the toxicity of zinc-finger nucleases. *Nat. Biotechnol.* **25**, 786–793 (2007).

ONLINE METHODS

Rat work in this study was performed at SAGE Labs, which operated under approved animal protocols overseen by SAGE's Institutional Animal Care and Use Committee (IACUC). Mouse work in this study was a contracted service provided by Maine Medical Center Research Institute (MMCRI) transgenic and gene targeting core facility, which operated under approved animal protocols overseen by MMCRI's IACUC.

ZFN constructs. The design and assembly of ZFNs were described previously[11,18]. The obligate-heterodimer form of ZFNs was used throughout[25]. Full ZFN amino acid sequences and DNA sequences are provided in **Supplementary Methods**. ZFN binding sites below are underlined, and the spacers between the binding sites are in bold. The same pair of ZFNs was used to target both the mouse and rat *Mdr1a* loci due to sequence conservation.

Mdr1a: 5′-GCCATCAGCCCT**GTTCTT**GGACTGTCAGCTGGT
CGGTAGTCGGGA**CAAGAA**CCTGACAGTCGACCA-5′
PXR: 5′-CAAATCTGCCGTGTA**TGTGGG**GACAAGGCCAATGGCT
GTTTAGACGGCACAT**ACACCC**CTGTTCCGGTTACCGA-5′

Donor construction. Homologous arms were PCR amplified from FVB mouse or Sprague Dawley rat genomic DNA. The primers used are listed in **Supplementary Table 1**. All donors used pBluescript SK (+) backbone (Stratagene). In NotI donors, left arms were cloned into KpnI and NotI sites, and right arms, NotI and SacII sites. GFP donors were constructed by inserting the PCR-amplified PGK-GFP cassette into the NotI site in the respective NotI donors in either direction. Donor plasmid was purified using GenElute Endotoxin-Free plasmid maxiprep kit (Sigma) and quantified on a Nanodrop.

mRNA preparation for microinjection. ZFN constructs were linearized at the XbaI site. *In vitro* transcripts were generated using T7 MessageMax kit (Epicentre) and polyA tailing kit (Epicentre), following manufacturer's instructions, and precipitated with an equal volume of 5 M ammonium acetate by incubating on ice for 15 min followed by centrifugation at >15,000*g* at 4 °C for 15 min. Washed and dried RNA was dissolved in water, and concentration was determined using a Nanodrop. mRNA is then transfected to cultured cells to validate activity using mutation detection assay.

Mutation detection assay. Sequencing primers were used in pairs to amplify a 300–400 bp region surrounding the target site. Ten microliters of each PCR product was then incubated using the following program: 95 °C, 10 min, 95 °C to 85 °C, at −2 °C/sec, 85 °C to 25 °C at −0.1 °C/sec. One microliter each of nuclease S and enhancer (Transgenomic) was added to digest the above reaction at 42 °C for 20 min. The mixture is resolved on a 10% polyacrylamide TBE gel (Bio-Rad).

Microinjection of fertilized eggs. At SAGE Labs, Sprague Dawley rats purchased from Charles River Laboratories were housed in standard cages and maintained on a 12 h light/dark cycle with *ad libitum* access to food and water. Four- to five-week-old donors were injected with 20 units of pregnant mare serum gonadotropin (PMS) followed by 50 units of human chorionic gonadotropin (hCG) injection after 48 h and again before mating. Fertilized eggs were harvested a day later for injection. ZFN mRNA and donor DNA were mixed and injected into the pronucleus of fertilized eggs. The final concentration of each ZFN mRNA was 2.5 ng/μl, and that of donor DNA was 1 ng/μl. Recipients were injected with 40 μg of LH-Rh 72 h before mating. Microinjected eggs were transferred to pseudopregnant Sprague Dawley recipients.

At MMCRI, FVB/NTac mice were housed in static cages and maintained on a 14 h and 10 h light/dark cycle with *ad libitum* access to food and water. Three- to four-week-old females were injected with 5 units of PMS and 48 h later, with 5 units of hCG. Fertilized eggs were harvested 10–12 h after hCG injection for microinjection. ZFN mRNA and donor DNA were mixed and injected into the pronucleus of fertilized eggs. Each ZFN mRNA was at a final concentration of 1 ng/μl, and the donor DNA at 2 ng/μl. Microinjected eggs were transferred to pseudopregnant Swiss Webster (SW) recipients, which receive 40 μg of LH-Rh injection 72 h before mating.

PCR and NotI digestion conditions. QuickExtract (Epicentre) was used to extract DNA from tail or toe clips, following manufacturer's instructions. Accuprime High Fidelity Taq polymerase (Invitrogen) was used in all PCR reactions with cycling conditions recommended by the manufacturer. NotI digestion was done by adding 1 μl 10× BSA and 1 μl NotI to 8 μl of PCR reaction and incubating at 37 °C for 2 h.

Preparation of genomic DNA for Southern blot analysis. Tail clips or ear notches were used to prepare genomic DNA for Southern blot analysis. Tissues were first incubated in lysis buffer (100 mM Tris-HCl, pH 8.8; 50 mM EDTA, 0.5% SDS; 200 mM NaCl; 300 μg/ml proteinase K) at 55 °C for 2 to 5 h with occasional inversions. Supernatant was collected and precipitated. The washed and dried pellet was then dissolved in TE buffer (10 mM Tris-HCl, pH 8.0, 1 mM EDTA).

Probe labeling. The probes were labeled with PCR DIG Probe Synthesis Kit (Roche) with Sprague Dawley rat genomic DNA as template and primers listed in **Supplementary Methods.**

Southern blot analysis. Fifteen micrograms of genomic DNA was digested for 3 h to overnight at 37 °C with PciI (*Mdr1a*) or PvuII (*PXR*), concentrated by precipitation and resolved on a 0.8% agarose gel. Upon transfer to nylon membrane and UV cross-linking (120,000 μJ/cm^2), prehybridization and hybridization were carried out according to instructions for DIG Easy Hyb Granules (Roche) at 42 °C (GFP probe) or 37 °C (PXR or Mdr1a probes). The membrane was then developed using DIG Detection Kit (Roche), following manufacturer's instructions. The developed membrane was exposed to a ChemiDocXRS+ Imaging system (BioRad).

Visualizing GFP in founder rats. BlueStar high intensity LED flashlight and BlueBlock filter glasses (Nightsea) were used to visualize GFP expression in the *Mdr1a* and *PXR* GFP founder rats.

doi:10.1038/nbt.1731